PROGRESS IN COLOR, COLORANTS AND COATINGS

available online @ www.pccc.icrc.ac.ir

Prog. Color Colorants Coat. 15 (2022), 191-202

Ministry of Science, Research and Technology
Institute for Color Science and Technology

Electrical Conductivity and Surface Morphology of PVB Films Doped with Different Nanoparticles

R. M. Omer[1], E. T. B. Al-Tikrity[1], R. N. Abed[*2], M. Kadhom[3], A. H. Jawad[4], E. Yousif[5]**

[1.] Department of Chemistry, College of Science, Tikrit University, P. O. Box: 34001, Tikrit, Iraq.

[2.] Mechanical Engineering Department, Engineering College, Al-Nahrain University, P. O. Box: 64040, Baghdad, Iraq.

[3.] Department of Environmental Science, College of Renewable Energy and Environmental Science, Alkarkh University of Science, P. O. Box: 31020, Baghdad, Iraq.

[4.] Faculty of Applied Sciences, University Teknology MARA, Shah Alam, P. O. Box: 40450, Selangor, Malaysia.

[5.] Department of Chemistry, College of Science, Al-Nahrain University, P. O. Box: 64021, Baghdad, Iraq.

ARTICLE INFO

Article history:
Received: 23 Apr 2021
Final Revised: 10 Aug 2021
Accepted: 14 Aug 2021
Available online: 27 Nov 2021

Keywords:
Poly (vinyl butyral)
PVB nanocomposite films
Dielectric constant
Electrical conductivity
Surface morphology.

ABSTRACT

Multiple poly (vinyl butyral) (PVB) nanocomposites films embedded with Co_3O_4,CuO, NiO, TiO_2, and Cr_2O_3 nanoparticles (NPs) were prepared using the casting method. Loading ratios of 0.001 wt.% of the nanoparticles were used in films preparation and the process was conducted at room temperature. The electrical properties of PVB nanocomposites films were analyzed at a frequency of 1-3 MHz. These properties included the dielectric constant (real and imaginary parts (Ɛ' and Ɛ'', respectively)), conductivity (ϬAC), loss factor (tan δ), surface energy loss function (SELF), and volume energy loss function (VELF). These variables showed a significant improvement once the films were filled with the NPs comparing with the blank PVB. Furthermore, a surface morphology examination for the PVB nanocomposites films was conducted using the field emission scanning electron microscopy (FESEM) and energy dispersive x-ray (EDX) spectroscopy. Overall, findings revealed that PVB nanocomposite films showed a higher conductivity compared to the PVB blank. Thus, this type of nanocomposite films could be utilized in photovoltaics, optical devices, and military apparatuses due to their extraordinary features, such as the radiation resistivity. Prog. Color Colorants Coat. 15 (2022), 191-202© Institute for Color Science and Technology.

1. Introduction

Poly(vinyl butyral) can act as an essential framework of composites that participate in different applications and industries due to its exceptional specifications. This polymer is generally a resin utilized in applications that demand flexibility, strong binding, toughness, and optical clarity. PVB is a random copolymer prepared by strengthening and reacting the poly(vinyl alcohol) (PVA) with butyraldehyde in an acidic medium, though significant quantities of unreacted vinyl alcohol are typically left within the chain [1]. Here, PVB is considered a reciprocal between vinyl-butyral and vinyl-alcohol co-polymers due to the combination between the polar and hydrophilic vinyl alcohol units and hydrophobic vinyl butyral units [2]. The PVB is commonly used in safety glass, paint due to the combination of transparency and mechanical strength, laminated binders, automobile windshields, and amorphous thermoplastic [3]. This

*Corresponding author: *rasheed.n.abed@nahrainuniv.edu.iq
** emad.yousif@nahrainuniv.edu.iq

wide window of applications is a result of its plasticity, resistance to atmospheric conditions (heat, humidity, rain), and adhesiveness to glass and metals. Furthermore, PVB thin films are also utilized in construction as a laminated glass for safety and security and in the photovoltaic industry to improve the durability of solar cell. Nevertheless, during the extrusion, PVB interlayers are exposed to elevated temperatures [4]. High temperatures cause a degradation in the structure due to the poor thermal stability of PVB resin, which makes the yellow interlayers and results in a distasteful odor [5]. Composite materials are combinations of two, or more, various materials that are expected to show advanced features that emerge from each element's properties. The composite properties are supreme to those of individual components. Talking about polymers, it was reported that new composites have high specific modulus and strength compared to the raw plastics, and their properties can be adapted in sophisticated applications [6]. Nanocomposites are classified as multi-phase solid materials in comparison to traditional composites, where one of the phases is a nanomaterial that sizes 1-100 nm in minimally one dimension [7]. These nanocomposites have good optical properties for light absorption that differ from the plain composite due to the change in the energy gap. Because of the nano-size of the additives, the nanocomposites have unique sizes and properties that conventional micro-composites do not typically own. The nanocomposites have applications in numerous fields; it has been estimated that the trend of global nanocomposites consumption will greatly increase over the next few years [8]. Modifying the PVB yields a proper material for additional applications of optoelectronic system that requires transparency, display, mechanical strength, and natural resistance for temperature changes [29].

In the current work, PVB was synthesized by reacting poly (vinyl alcohol) in an acidic medium with butyraldehyde to produce the basic composite, which was filled with nanoparticles in an advanced step. The nanoparticles addition step was conducted to modify and improve the surface morphology toward light absorption and the electrical conductivity for the composite. The conductivity (ϭAC), dielectric constant (ε^*), loss factor (tan δ), surface energy loss function (SELF), and volume energy loss function (VELF) were computed through this work. The surface morphology of PVB nanocomposite films was also investigated by utilizing FESEM and EDX devices to exhibit the nanoparticles distribution through PVB films' textures. To our knowledge, there is no previous work for doping Poly (vinyl butyral) by the nanomaterials.

2. Experimental

2.1. Materials

PVA of purity 98 % and molecular weight (M wt.) of 72,000 $g.mol^{-1}$ and butyraldehyde of purity 99 % and (M wt.) of 72.11 $g.mol^{-1}$ were imported from AppliChem company (Germany). The combination of these two materials led to the synthesis of composite films that were embedded with NPs to generate the nanocomposite films. Nanoparticles of Co_3O_4, CuO, NiO, TiO_2, and Cr_2O_3 that sized around 15.1, 56.4, 30.7, 48.8, and 18.5 nm, respectively, were supplied from Sigma Aldrich Company (Germany). These nanoparticles were consequently examined by the atomic force microscope (AFM) as described in our previous work [9].

2.2. Synthesis and preparation of PVB/NPS composites films

PVB polymer was prepared according to a determined protocol [10]. Methanol was added to PVB solution and stirred for 60 min at 50 °C; nanoparticles of Co_3O_4, CuO, NiO, TiO_2, and Cr_2O_3 of a concentration 0.001 wt.% were added to the PVB solution [9]. Then, these mixtures were placed in an ultrasonic bath for 50 min. Finally, the mixtures were cast on a substrate of glass, and the formed films were left to dry at 28 °C for 36 h under vacuum, the synthesis of the PVB nanocomposite films was agreed with the same method of synthesis in paper [10]. Scheme 1 shows the preparation process.

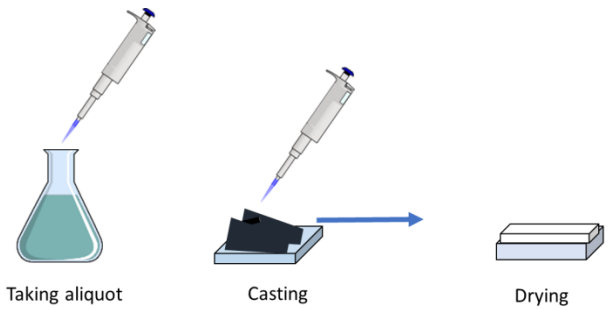

Scheme 1: PVB nanocomposite films preparation process.

2.3. Characterization of systems

An electronic LCR testing tool of model 4274A from Hewlett-Packard was employed for measuring the inductance (L), capacitance (C), and resistance (R). The surface morphology of PVB films was inspected using a FESEM, TESCAN MIRA3, (Kohoutovice, Czech Republic) at an accelerating voltage of 10 kV. While PVB nanocomposite films' depth was identified as 50 µm utilizing a Digital Vernier Caliper 2610 micrometer tool. Energy-dispersive X-ray spectroscopy (EDX) measurements were performed using the Bruker X-Flash (R) 6|10 detector (Tokyo, Japan), as the same inspection agreed with others' work [9]. The pictures of microscope were taken by the optical texture observation using MEIJI microscope equipped with INSTEC hot stage and central processor controller mK1000, and connected with Lumenera color video camera.

3. Results and Discussion

3.1. Dielectric constant measurements with LCR Meter

The dielectric constant was graphed versus the frequency that was measured at various limitations of the PVB nanocomposite films as shown in Figures 1 and 2. The permittivity variation of the nanocomposites was clarified as a relation with the frequency of dielectric parameters as listed in equation 1 [11] by utilizing a LCR meter of a frequency range 1-3 MHz:

$$(\varepsilon^{*}) = \varepsilon'(\omega) + i\,\varepsilon''(\omega)\ldots \quad (1)$$

Where Ɛ* is the main dielectric constant, Ɛ' is the dielectric constant real part, and Ɛ" is the imaginary part. The blank and nanocomposite PVB films were cut to pieces, each piece has a dimension (2 × 1.5 cm), in dry conditions to be prepared for the silver electrode test. This preparation is to ultimately determine the real and imaginary parts of dielectric permittivity of the nanocomposite samples, then to facilitate the measurement of the alternative current (AC) conductivity properties [12].

3.2. Real and imaginary of dielectric constants

The real and imaginary parts are denoted by Ɛ' and Ɛ", respectively, which were estimated for each cycle of the electrical field, where these constants referring to the energy storage.

The real part can be computed for the PVB nanocomposite films from equation 2 [12]:

$$\varepsilon' = \frac{Cd}{\varepsilon^{\circ}A} \ldots \quad (2)$$

Where, C is the capacitance constant which can be measured by the apparatus, d is the film's thickness (between two electrodes), A is the electrode's area, and Ɛ is the space permittivity (8.85×10^{-12} F.m^{-1}). The results of the real part are shown in Figure 1 [12].

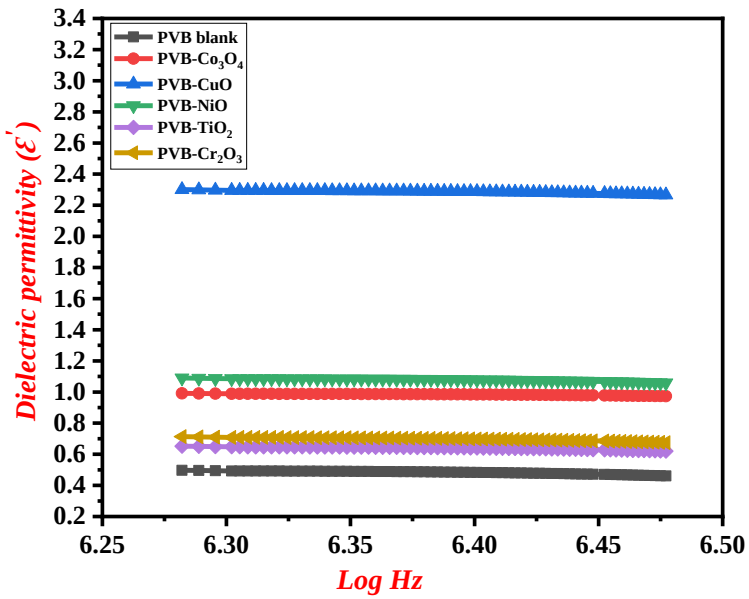

Figure 1: The real part of dielectric constant (Ɛ') relationship with logarithm of frequency for different nanoparticles oxides that were embedded with PVB nanocomposite films at room temperature.

It is obvious from Figure 1 that the real part of the dielectric constant decreased slightly along with the increase in logarithmic values of the frequency. The dielectric dispersion may illustrate the interchange of electrons among the PVB nanocomposite films. This generates holes, and a movement happens through the energy gap between the valence and conduction bands of the semiconductor material [13].

The imaginary part of the dielectric relationship with the logarithm of frequency was presented in Figutre 2, where this part can be computed from equation 3 [13]:

$$\varepsilon'' = \varepsilon' \times \tan\delta \ \ldots \quad (3)$$

Hence, ε'' is the imaginary part of the dielectric constant, ε' is the real part of the dielectric constant, and $\tan\delta$ is the loss factor of dissipation.

It can be seen that the imaginary part of the dielectric constant (Ɛ") declines gradually along with the frequency increase. This reduction is usually associated with the decrease in energy bonds among electrons [14].

3.3. Electrical conductivity

The electrical conductivity has remarkably increased by dispersing the nanomaterials in the PVB films. This improvement indicates that the distance among electrons plays a significant role in charges transfer through the bands (valence and conduction) [15]. The electrical conductivity can be computed from the real and imaginary parts of the dielectric constant, with a loss factor for the blank and nanocomposite PVB films as shown in equation 4 [16]:

$$6 = \varepsilon_o \varepsilon' \omega \tan\delta \ldots \quad (4)$$

Where, 6Ac is the conductivity of the alternative current, ε_o is the angular frequency, $\omega=2\pi f$, where f is the applied frequency to compute real dielectric loss, and tan δ is the loss factor.

Here, the conductivity (ƆAc), dielectric permittivity (ε'), imaginary permittivity (ε"), and loss factor (tan δ) of PVB nanocomposite films filled with 0.001 wt.% of Co_3O_4, CuO, NiO, TiO_2, and Cr_2O_3 were measured with frequency. The results of the electrical conductivity were drawn versus the frequency logarithm as shown in Figure 3. The frequency effect on the electrical properties was studied in the range 1-3 MHz for the blank and nanocomposite PVB films. This figure shows the associated relationship between the NPs and PVB particles through the dispersion of NPs. Thereby, enhancing the conductivity by frequency increasing is attributed to the hops of charge carriers between bands due to the motivation of charge carriers through the conduction band [17].

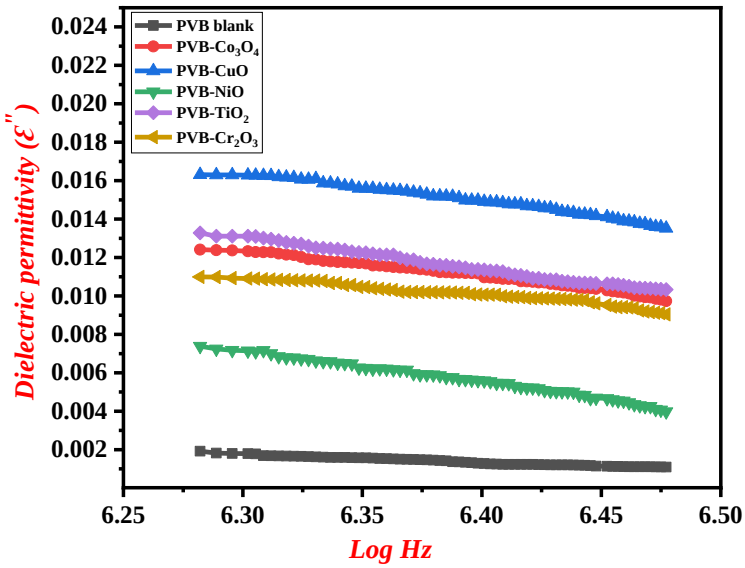

Figure 2: Imaginary part of dielectric permittivity (Ɛ") relationship with logarithm of frequency for different nanoparticles that were filled in the nanocomposite films at room temperature.

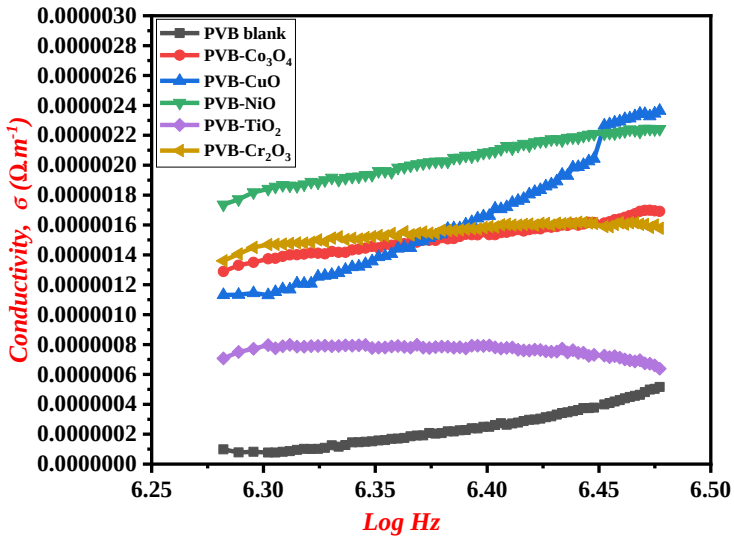

Figure 3: Conductivity (σ) for different nanoparticles of PVB nanocomposite films in different frequencies at room temperature.

The electrical conductivity of PVB nanocomposite films has gradually increased by increasing the frequency. Certainly, it can be observed that PVB's dielectric permittivity increased by mixing with the nanomaterials. Nevertheless, the conductivity of PVB nanocomposite films showed a slow increase with frequency increasing when equal amounts of the nanoparticles were used [18]. However, the electrical conductivity increase followed the below order: pure PVB<PVB+TiO_2<PVB+Co_3O_4<PVB+Cr_2O_3<PVB+CuO< PVB+NiO

The change in PVB nanocomposite films' electrical conductivity in Figure 3 displays the dependence on the frequency. From the figure, CuO and NiO PVB nanocomposite films had the highest conductivity, while the lowest was for the TiO_2 nanocomposite film. These results are in good agreement with previous findings [19].

3.4. Dielectric loss factor

The energy loss inside PVB nanocomposite films is determined by the dielectric loss factor (tan δ), which represent the phase change due to implement specific frequency. The dielectric loss factor can be commonly utilized in any dielectric material as a measure of energy dissipation through the PVB nanocomposite films, and computed from equation 5 [20]:

$$\tan\delta = \frac{\varepsilon''}{\varepsilon'} \ldots \quad (5)$$

Where all parameters were defined above.

Here, when the frequency is applied on the PVB nanocomposite films, it causes a vibration in the structure that leads to the dipole's relaxation and free rotation. This results in ions jumping through the valence and conduction bands and creates the electrical conductivity; thereby, the dielectric loss factor will be created [21]. The loss factor relationship with the frequency was drawn in Figure 4.

From Figure 4, it can be noted that tan δ decreases as the frequency increases. Moreover, the values of tan δ for PVB nanocomposite films had further reduction after adding the nanoparticles to the polymer structure. This led to minimizing the energy dissipation and confirming that these nanomaterials decrease the loss factor of the films [22].

3.5. Surface and volume energy loss factors

Energy dissipation occurs by the fast movement of electrons when passing through the bands [18]. The surface and volume energy loss factors are correlated with the fast movement of electrons when they lose their energy after traveling within the material and on its surface. The surface energy loss function (SELF) and volume energy loss function (VELF) are correlated with real and imaginary parts ε' and ε'' of the dielectric constant. These parameters can be computed from these equations (Eq. 6 and 7) [23]:

$$\left[\mathrm{SELF}=\frac{\varepsilon''}{\left(\varepsilon'^{2}+\varepsilon''^{2}\right)}\right]\ldots \quad (6)$$

and

$$\left[\text{VELF}=\frac{\varepsilon'}{\left(\varepsilon'+1\right)^{2}+\varepsilon''^{2}}\right]\ldots \quad (7)$$

Where, SELF and VELF are the surface and volume energy loss factors, respectively.

As demonstrated above, SELF decreases gradually as the frequency increases along the axis. The SELF values decreased by adding the nanoparticles to PVB structures as shown in Figure 5 because SELF depends on the values of ε' and ε'' that has similar behavior of ε' and ε'' when they were examined with the frequency.

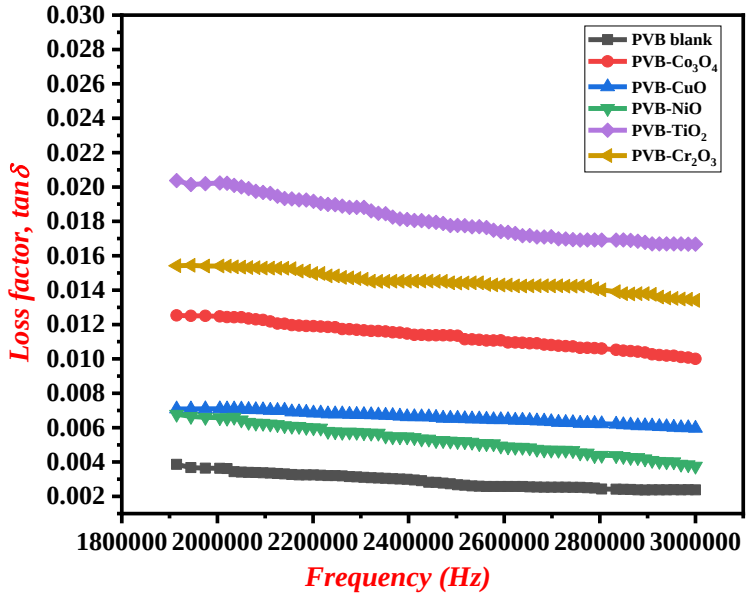

Figure 4: Dielectric loss factor (tan δ) of different PVB nanocomposite films relationship with frequency at room temperature.

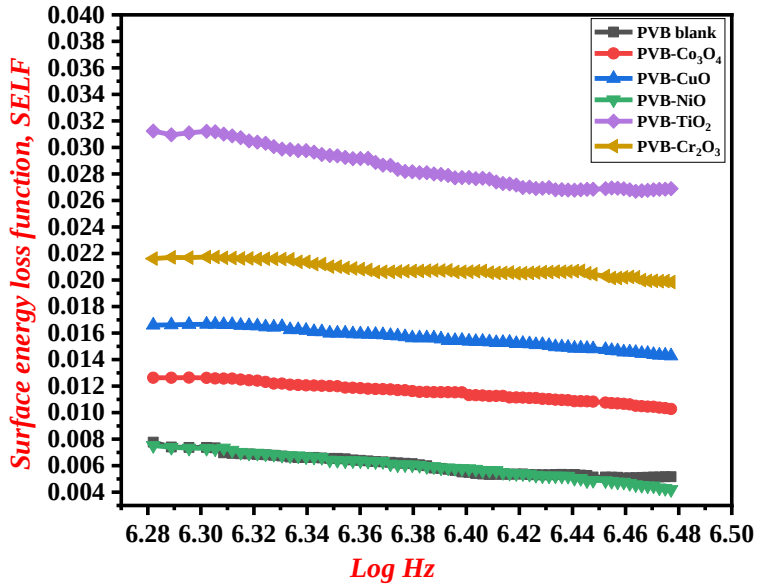

Figure 5: SELF relationship with frequency logarithm of different PVB nanocomposite films at room temperature.

Likewise, VELF decreases gradually with frequency increase. Also, the VELF values furtherly decreased by adding the nanoparticles to the PVB lattice as shown in Figure 6. Similar to the SELF. The VELF parameter depends on the square values of ε' and ε'' of the dielectric constant in the denominator [24].

These results are in good agreement and similar to the curve of dielectric constant results. Therefore, inside the PVB nanocomposite films, the energy lose happens for the free charge transporters and becomes higher than the free carriers that traverse the surface [25].

3.6. Analysis of FESEM and microscope images

The blank and nanocomposite PVB films' images were captured by the FESEM and microscope as clarified in Figure 7 a and b, respectively. The morphology of all films' surfaces was examined using a magnification range of 10 to 300.00 Kx. Images of Figure 7a demonstrate a rough surface of all films with a scale bar of 200 nm, where a change in the morphology is noticed after filling the nanoparticles. This change is expected due to the variation in the overall physicochemical properties of the polymer [24]. Filling the NPs shows a change in the morphology, where each additive has influenced the properties variously.

The microscope images (400X magnification) in Figure 7b of all films exhibit the existence of small troughs on the surface. Also, the surface was rough and the change in color underwent the effect of microscope light. From a viewpoint, the presence of surface roughness leads to show dark places as a result of blocking light from them [25].

3.7. EDX analysis

The spectroscopy analysis of EDX was employed as a powerful technique to get the basic chart of PVB film as shown in Figure 8. From the figure, a homogeneous surface of the PVB polymer can be recognized and the atomics in the film were similar. However, change in the films' morphology can be recognized after filling the nanoparticles due to the change in the properties [26-28]. It is obvious from the EDX analysis that all the elements of samples were appeared as peaks in the analysis of pure PVB and PVB were doped with NPs. In Figure 8, there is a homogenous mixing for the pure PVB is appeared in it [29, 30].

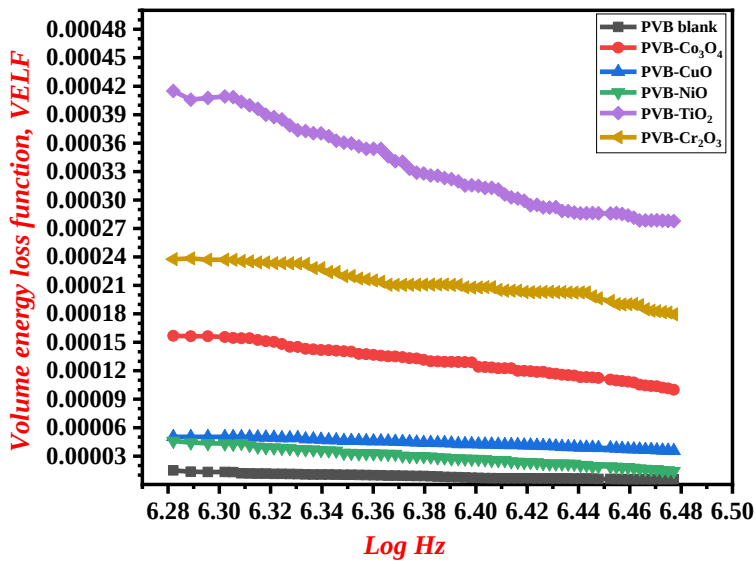

Figure 6: VELF relationship with frequency logarithm of different PVB nanocomposite films at room temperature.

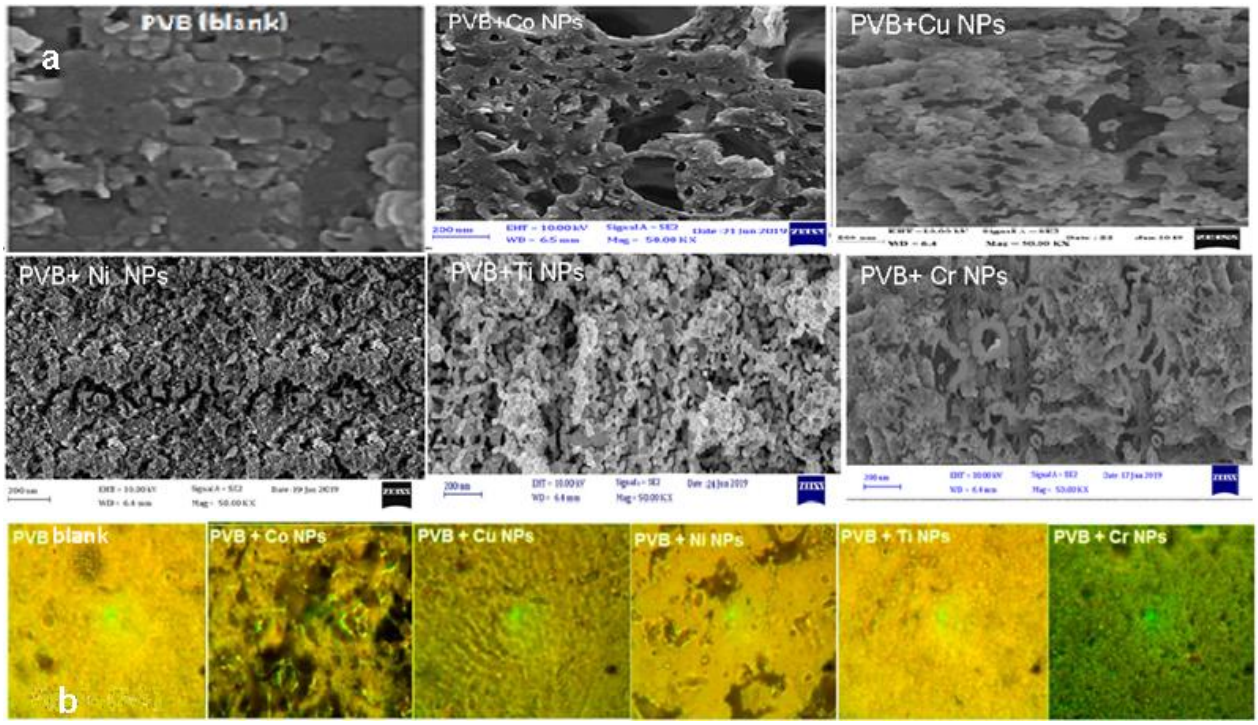

Figure 7: (a) FESEM images of blank and nanocomposite PVB films, and (b) microscope images of blank and nanocomposite PVB films with 400X magnification.

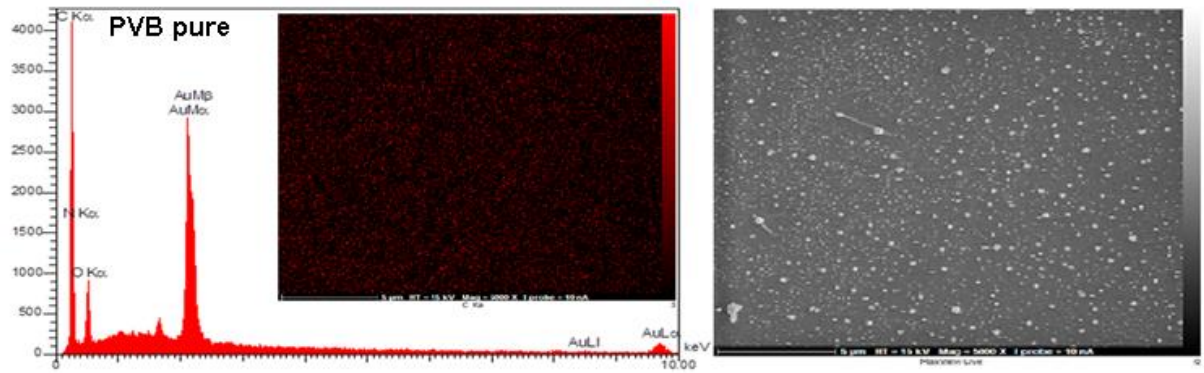

Figure 8: EDX spectra of pure PVB film.

The spectroscopy analysis of EDX for the PVB nanocomposite films showed a robust absorption band, where the nanocomposite films of Co_3O_4, CuO, NiO, TiO_2, and Cr_2O_3 are shown in Figure 9a, b, c, d, and e, respectively. These tests confirmed filling the nanocomposites films structure was successful, hence the Information from the images showed growth surface films depending on the concentration of the NPs are embedded with the PVB matrix. Whereas, the dispersion of the NPs with different concentrations indicates the incorporation of the NPs in the PVB polymer matrix gives validating results about EDX measurements [31, 32].

EDX elemental analysis of the polymers containing nanocomposite materials chart has shown the appearance of new peaks at 6.9, 8.05, 7.4, 4.5, and 5.5 keV corresponding to Co_3O_4, CuO, NiO, TiO_2, and Cr_2O_3, respectively as appears in Figure 9 (a-e). Despite the EDX elemental analysis is doesn't give a quantitative description of the data, but it can give information about the surface of the polymers where oxygen peak is significantly increased in comparison to the original peak in the pure PVB polymer. This change can be attributed to the increase in the oxygen concentration that comes from the nanofillers oxide form [32].

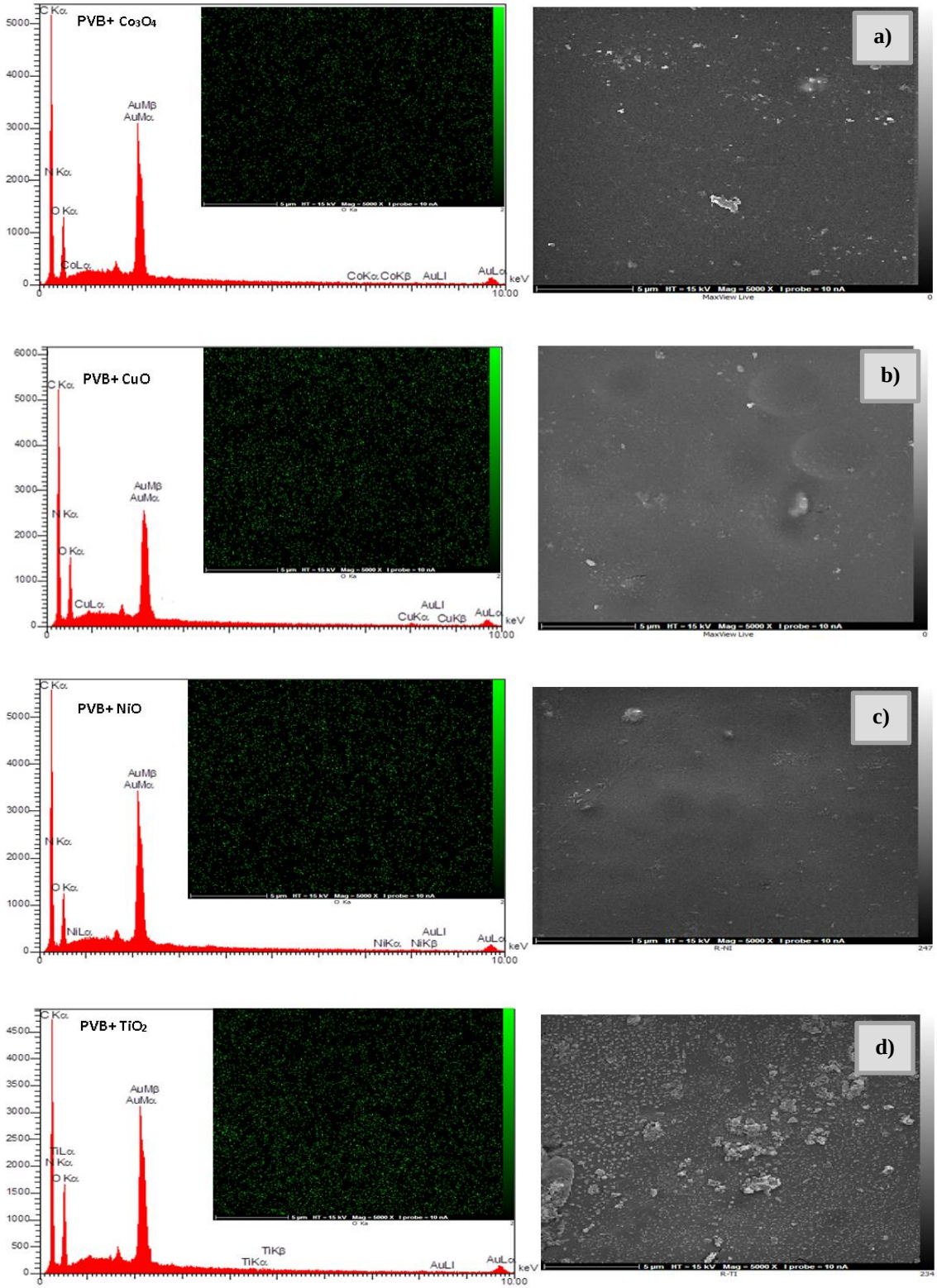

Figure 9: EDX spectra of PVB films filled with different nanoparticles; a) PVB+CO_3O_4, b) PVB+CuO, c) PVB+NiO, d) PVB+TiO_2 and e) PVB+Cr_2O_3.

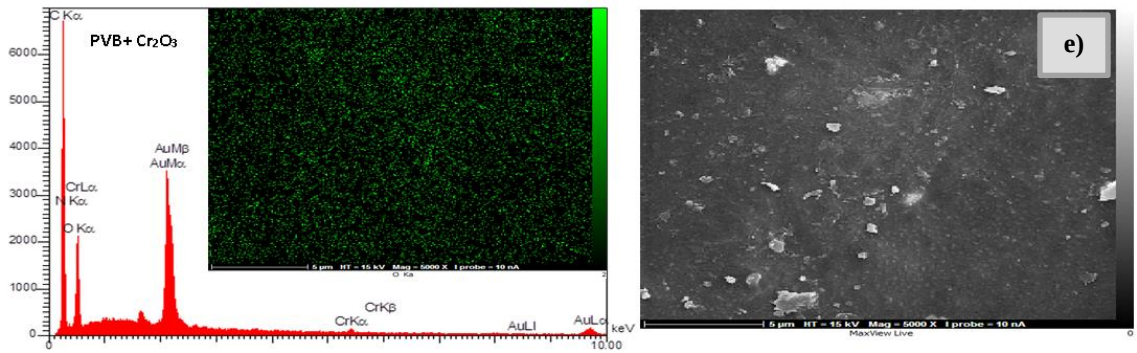

Figure 9: continue.

4. Conclusion

Poly(vinyl butyral) films filled with different nanoparticles were synthesized using the casting method. Nanoparticles of Co_3O_4, CuO, NiO, TiO_2, and Cr_2O_3 were selected and mixed with the PVB casting solution by blending in a concentration of 0.001 wt.% at 50 °C for 1 h. The PVB nanocomposites films were analyzed for electrical properties at a frequency of 1-3 MHz. The electrical properties included the dielectric constant permittivity (real (Ɛ') and imaginary (Ɛ") parts), conductivity (ϬAC), loss factor (tan δ), surface energy loss function (SELF), and volume energy loss function (VELF). These variables were found to be more significant for the PVB nanocomposites films comparing with the blank PVB. The results showed higher electrical conductivity of PVB/CuO and PVB/NiO nanocomposite films comparing with other types, which have strong conductivity compared with others. However, these conducted lower values of dielectric loss factor surface (tan δ), energy loss function (SELF), and volume energy loss function (VELF). All the above parameters decrease with adding the NPs to the PVB lattice and reinforce the structure toward the conductivity except for the conductivity (ϬAC). The surface morphology of PVB nanocomposites films was examined by the FESEM showed good distribution of the NPs through the PVB lattice; furthermore, the energy EDX spectroscopy was conducted. Overall, findings revealed that PVB nanocomposite films performed a higher conductivity compared with the PVB blank**.** Based on this work outcomes, it was found that filling the NPs within the PVB matrix has improved the total physicochemical properties, which promise a wider application of this polymer.

Acknowledgments

The authors like to thank the Department of Chemistry, College of Science and Department of Mechanical Engineering, College of Engineering at Al-Nahrain University for partially supporting this work.

5. References

1. F. Shen, X. Lu, X. Bian and L. Shi, Preparation and hydrophilicity study of poly(vinyl butyral)-based ultrafiltration membranes, *J. Membr. Sci.*, 265(2005), 74-84.
2. W. Z. Lang, J. P. Shen, Y. X. Zhang, Y. H. Yu, Y. J. Guo, C. X. Liu, Preparation and characterizations of charged poly(vinyl butyral) hollow fiber ultrafiltration membranes with perfluorosulfonic acid as additive, *J. Membr. Sci.*, 430(2013), 1-10.
3. M. Hajian, M. R. Reisi, G. A. Koohmareh, A. R. Z. Jam, Preparation and characterization of Polyvinylbutyral/Graphene Nanocomposite, *J. Polym. Res*, 19(2012), 1-7.
4. J. C. Hoepfner, M. R. Loos, S. H. Pezzin, Evaluation of thermomechanical properties of polyvinyl butyral nanocomposites reinforced with graphene nanoplatelets synthesized by in situ polymerization, *J. Appl. Polym. Sci.*, 135(2018), 46157 (1-10).

5. W. Wang, S. Guan, M. Li, J. Zheng, C. Xu, A novel hybrid quasi-solid polymer electrolyte based on porous PVB and modified PEG for electrochromic application, *Org. Electron.*, 56(2018), 268-275.
6. S. Pizzanelli, C. Forte, S. Bronco, T. Guazzini, C. Serraglini and L. Calucci, PVB/ATO Nanocomposites for Glass Coating Applications: Effects of Nanoparticles on the PVB Matrix, *MDPI Coat.*, 9(2019), 247(2-16)
7. M. M. L. Sonia, S. Anand, S. Blessi, S. Pauline, A. Manikandan, Effect of surfactants (PVB/EDTA/CTAB) assisted sol-gel synthesis, structural, magnetic and dielectric properties of $NiFe_2O_4$ nanoparticles, *Ceram. Int.*, 44(2018) 1-40
8. Z. Hussain, G.A. El-Hiti, A. Ahmed, N. Altaee, E. Yousif, Photocatalytic Degradation of Polyhydroxy-butyrate Films Using Titanium Dioxide Nanoparticles as a Photocatalyst, *Russ. J. Appl. Chem.*, 89(2016), 1536−1543
9. R. M. Omer, E. Yousif, E.T. B. Al-Tikrity, D. S. Ahmed, A. A. Ali, R. N. Abed, A Detailed Examination of UV Radiation Effects on the Structural and Morphological Properties of Polyvinyl Butyral Films Containing Different Nanoparticles, *Prog. Color Colorants Coat.*, 14 (2021), 209-219
10. Ghazi, D.; El-Hiti, G. A.; Yousif, E.; Ahmed, D. S.; Alotaibi, M. H., The Effect of Ultraviolet Irradiation on the Physicochemical Properties of Poly(vinyl Chloride) Films Containing Organotin(IV) Complexes as Photostabilizers. *Molecules*, 23(2018), 254,1-15.
11. A. K. Bajpai, J. Bajpai, & S. N. Soni, Preparation and characterization of electrically conductive composites of poly (vinyl alcohol)-g-poly(acrylic acid) hydrogels impregnated with polyaniline (PANI), *EXPRESS Polym. Lett.*, 2(2008), 26-39
12. S. M. H. Bukhari, S. Khan, M. Rehanullah, N. M. Ranjha, Synthesis and Characterization of Chemically cross-linked acrylic acid/gelatin hydrogels: effect of ph and composition on swelling and drug release, *Inter. J. Poly. Scie.*, (2015), 1-15
13. S. Nagaveena, C. K. Mahadevan, Preparation by a facile method and characterization of amorphous and crystalline nickel sulfide nanophases, *J. All. Comp.*, 582(2014), 447-456
14. S. I. S. Ramya, C. K. Mahadevan, Preparation and structural, optical, magnetic, and electrical characterization of $Mn^{2+}/Co^{2+}/Cu^{2+}$ doped hematite nanocrystals, *J. Solid State Chem.*, 211(2014), 37-50
15. N. Ni, K. Zhao, Dielectric analysis of chitosan gel beads suspensions: Influence of low crosslinking agent concentration on the dielectric behavior, *J. Colloid Interface Sci.*, 312(2007), 256–264.
16. V. S. Sangawar, R. J. Dhokne, A. U. Ubale, P. S. Chikhalikar, S. D. Meshram, Structural characterization and thermally stimulated discharge conductivity (TSDC) study in polymer thin films, *Bull. Mater. Sci*., 30(2007), 163-166.
17. S. P. Mondal, R. Aluguri, S. K. Ray, Dielectric and transport properties of carbon nanotube-CdS nanostructures embedded in polyvinyl alcohol matrix, *J. Appl. Phys.*, 105(2009), 114317 (1-8).
18. A. S. Hassanien, Studies on dielectric properties, opto-electrical parameters and electronic polarizability of thermally evaporated amorphous $Cd_{50}S_{50}$-xSe_x thin films, *J. All. Comp.*, 671(2016), 566-578.
19. J. B. Kana, J. M. Ndjaka, G. Vignaud, A. Gibaud, M. Maaza, thermally tunable optical constants of vanadium dioxide thin films measured by spectroscopic ellipsometry, *Opt. Commun.*, 284(2011), 807-812.
20. H. E. Atyia, N. A. Hega, Optical spectroscopy and dispersion parameters of $Ge_{15}Se_{60}X_{25}$ (X = As or Sn) amorphous thin films, *Eur. Phys. J. Appl. Phys.*, 63(2013), 10301(p1-p7).
21. A. M. Abd-Elnaiema, S. Moustafaa, A. M. Abdelraheem, M. A. Abdel-Rahim, A.Z. Mahmoud, Effects of annealing on structural and optical properties of Ge20Se70Sn10 thin films for optoelectronic applications, *J. Non-Cryst. Solids*, 549(2020), 120353 (1-10).
22. S. Sarkar, N. S. Das, K. K. Chattopadhyay, Optical constants, dispersion energy parameters and dielectric properties of ultra-smooth nanocrystalline BiVO4 thin films prepared by rf-magnetron sputtering, *Solid State Sci.*, 33(2014), 58-66.
23. H. E. Atyia, N. A. Hegab, Determination and analysis of optical constants for Ge15Se60Bi25 thin films, *Physica B: Condens. Matter*, 454 (2014) 189-196.
24. A. Pourjavadi, G. R. Mahdavinia, Super absorbency pH-sensitivity and swelling kinetics of partially hydrolyzed chitosan-g-poly(acrylamide) hydrogels, *Turk J. Chem.*, 30(2006), 595-608.
25. M. P. Kumar, T. Sankarappa, S. Kumar, AC conductivity studies in rare earth ions doped vanadotellurite glasses, *J. All. Comp.*, 464(2008) 393-398.
26. P. Kumar, N. Khan, D. Kumar, Polyvinyl butyral (PVB), versetile template for designing nanocomposite/composite materials: a review, *Gr. Chem. Tech. Lett.*, 2 (2016), 185-194.
27. T. Niratiwongkorn, G. E. Luckachan, V. Mittal, Self-healing protective coatings of polyvinyl butyral/polypyrrole-carbon black composite on carbon steel, *RSC adv.*, 6(2016), 43237-43249.
28. M. B. Povea, W. A. Monal, J. V. C. Rodríguez, A. M. Pat, N. B. Rivero, C. P. Covas, Interpenetrated chitosan-poly (acrylic acid-Co-acrylamide) hydrogels. synthesis, characterization and sustained protein release studies, *Mater. Scie. Appl.*, 2(2011), 509-520.
29. S. Dey, D. Mohan, G. C. Dhal, R. Prasad, Copper based mixed oxide catalysts (CuMnCe, CuMnCo and CuCeZr) for the oxidation of CO at low temperature, *Mater. Discov.*, 10(2017), 1-14.
30. S. Dey, G. C. Dhal, D. Mohan, R. Prasad, Structural and catalytic properties of Fe and Ni doping on $CuMnO_x$ catalyst for CO oxidation, *Adv. Compos. Hybrid Mater.*, 3(2020), 84-97.

31. S. Dey, G. C. Dhal, Property and structure of various platinum catalysts for low-temperature carbon monoxide oxidations, *Mater. Today Chem.*, 16(2020), 100228-1-100228-24.

32. R. Divya, M. Meena, C. K. Mahadevan and C. M. Padma, Investigation on CuO Dispersed PVA Polymer Films, *Int. J. Eng. Res. Appl.*, 4(2014), 1-7.

How to cite this article:
R. M. Omer, E. T. B. Al-Tikrity, R. N. Abed, M. Kadhom, A. H. Jawad, E. Yousif, Electrical Conductivity and Surface Morphology of PVB Films Doped with Different Nanoparticles. Prog. Color Colorants Coat., 15 (2022), 191-202.